

**AD-A281 381**



①

**In Situ Grown Quantum-Wire Lasers  
ARO #DAAL03-91-G-0134 - FINAL REPORT**

by

L. A. Coldren: Principal Investigator

A.C. Gossard: Co-Principal Investigator

J.H. English: Development Engineer

D. Mui: Post Doc

S.W. Corzine, S.Y. Hu, D.B. Young, T. Strand, R.

Herrick, S.-L. Lee: Students

ECE Technical Report #94-09

**DTIC**  
**ELECTE**  
**JUL 12 1994**  
**S B D**

**DISTRIBUTION STATEMENT A**  
**Approved for public release**  
**Distribution Unlimited**

378 94-21059

Department of Electrical & Computer Engineering

University of California at Santa Barbara

April 7, 1994

DTIC STATEMENT PROTECTED 1

**94 7 11 020**

REPORT DOCUMENTATION PAGE			Form Approved OMB No 0704-0188	
<small>Public reporting burden for this collection of information is estimated to average 1 hour per response, including the time for reviewing instructions, searching existing data sources, gathering and maintaining the data needed, and completing and reviewing the collection of information. Send comments regarding this burden estimate or any other aspect of this collection of information, including suggestions for reducing this burden, to Washington Headquarters Services, Directorate for Information Operations and Reports, 1215 Jefferson Davis Highway, Suite 1204 Arlington, VA 22202-4302 and to the Office of Management and Budget, Paperwork Reduction Project (0704-0188), Washington, DC 20503.</small>				
1. AGENCY USE ONLY (Leave blank)	2. REPORT DATE 4/7/94	3. REPORT TYPE AND DATES COVERED Final 15 May 91 - 14 Jan 94		
4. TITLE AND SUBTITLE  In Situ Grown Quantum-Wire Lasers		5. FUNDING NUMBERS  DAAL03-91-G-0134		
6. AUTHOR(S)  L.A. Coldren, Principal Investigator A.C. Gossard, Co-Principal Investigator				
7. PERFORMING ORGANIZATION NAME(S) AND ADDRESS(ES)  Dept. of Electrical & Computer Engineering University of California Santa Barbara, CA 93106		8. PERFORMING ORGANIZATION REPORT NUMBER		
9. SPONSORING/MONITORING AGENCY NAME(S) AND ADDRESS(ES)  U.S. Army Research Office P.O. Box 12211 Research Triangle Park, NC 27709-2211		10. SPONSORING, MONITORING AGENCY REPORT NUMBER  ARO 28922.14-EL-SOI		
11. SUPPLEMENTARY NOTES The views, opinions and/or findings contained in this report are those of the author(s) and should not be construed as an official Department of the Army position, policy, or decision, unless so designated by other documentation.				
12a. DISTRIBUTION/AVAILABILITY STATEMENT  Approved for public release; distribution unlimited.			12b. DISTRIBUTION CODE	
13. ABSTRACT (Maximum 200 words)  This program concentrated on developing techniques to better understand and fabricate quantum-confined structures. The goal was to create the enabling technology for more efficient semiconductor lasers and integrated optoelectronic circuits. Over the contract period, significant advances occurred in the development of quantum-confined lasers, UHV <i>in-situ</i> processing technology, and the underlying theory for quantum-confined laser structures. The quantum-confined laser work included both quantum-wire laser and vertical-cavity laser development. This latter effort also required substantial improvements in the MBE growth technology. Much of this technology is now ready for transfer to industry. In fact, a number of joint projects with industry are underway, as a result of this program.				
14. SUBJECT TERMS			15. NUMBER OF PAGES	
			16. PRICE CODE	
17. SECURITY CLASSIFICATION OF REPORT  UNCLASSIFIED	18. SECURITY CLASSIFICATION OF THIS PAGE  UNCLASSIFIED	19. SECURITY CLASSIFICATION OF ABSTRACT  UNCLASSIFIED	20. LIMITATION OF ABSTRACT  UL	

## Table of Contents

	Page
I Introduction.....	1
II MBE Growth .....	3
III Vertical Cavity Surface Emitting Laser Research .....	5
IV. Modelling for reduced threshold VCSELs .....	9
V. Quantum-wire lasers and Characterization .....	12
VI. <i>In-situ</i> etching and regrowth .....	13
1. Electrical quality of regrowth interface .....	13
2. Regrowth over etched structures .....	14
3. Surface morphology .....	15
4. Buried in-plane lasers .....	16
VII. Participating Scientific Personnel .....	17
VIII. Appendix I - Summary Foils from Technology Transfer workshop .....	18
IX. Appendix II - Publications resulting from ARO work .....	33

Accession For	
NTIS GRA&I	<input checked="" type="checkbox"/>
DTIC TAB	<input type="checkbox"/>
Unannounced	<input type="checkbox"/>
Justification	
By	
Distribution/Avail	
Availability Codes	
Dist	Avail and/or Special
A-1	

## ***I. Introduction***

This program concentrated on developing techniques to better understand and fabricate quantum-confined structures. The goal was to create the enabling technology for more efficient semiconductor lasers and integrated optoelectronic circuits. Over the contract period, significant advances occurred in the development of quantum-confined lasers, UHV *in-situ* processing technology, and the underlying theory for quantum-confined laser structures. The quantum-confined laser work included both quantum-wire laser and vertical-cavity laser development. This latter effort also required substantial improvements in the MBE growth technology. Much of this technology is now ready for transfer to industry as outlined in Appendix I. In fact, a number of joint projects with industry are underway, as a result of this program.

The work on quantum-wire lasers with 'serpentine superlattice' active regions has generated seminal results demonstrating optical gain anisotropy in in-plane ridge laser structures. This work also resulted in a novel technique of de-embedding the leakage current contribution in ridge laser structures. The vertical-cavity laser effort resulted in an improved theoretical understanding of expected performance as well as record breaking experimental characteristics, including temperature insensitive behavior, high output power, and reduced surface recombination.

The UHV *in-situ* processing work provided a much better understanding of the nature of interface traps that exist at MBE regrown interfaces. Improved etching and regrowth techniques resulted in interface state densities well below  $10^{11}/\text{cm}^2$  and nearly ideal Schottky diode characteristics for the first time. Also, successful *in-situ* etched mesa overgrowths have been carried out demonstrating low surface recombination and reduced threshold currents in mesa-etched lasers. This work continues under NSF funding in the direction of creating accurate quantum-wire structures using regrowth on etched sidewalls containing multiple quantum-wells.

The theoretical gain modelling work has generated an original theoretical treatment of quantum-confined structures that has been the basis of two book chapters, two invited papers, and a user-friendly highly-efficient software package[1-3, 13]. The package also includes

vertical-cavity laser design programs. This package has been transferred to engineers at Honeywell, AT&T and Hewlett-Packard. The gain software includes quantum-confinement as well as valence-band mixing and strain effects, and numerical analysis short cuts allows it to generate gain curves on a Macintosh in a few minutes.

## **II. MBE Growth**

During the course of the ARO contract, several improvements have been carried out on the Varian Gen II Molecular Beam Epitaxy system used for the growth of the structures under study in this contract. In the pursuit of higher uniformity growths, lower defect levels, and higher system uptime, a high capacity dual-zone gallium furnace was installed in the system. This furnace has a gallium capacity of nearly 3x the previous furnace, and has increased the amount of material that the system is capable of growing between source replenishments. We have also seen a reduction in flux transients at shutter openings due to the hot-lip configuration.

To improve the flexibility of the system, an inverted gallium cell was designed and implemented. Previously we were limited by the geometry of the MBE source configuration, which has only four upward-looking furnace positions. Prior to this source design, liquid sources were required to be in upward-looking positions so that the liquid was contained in the furnace crucible. This new cell design allows a low-capacity, low growth-rate gallium source to be installed in a downward-looking furnace position. This allows the system to be configured with five group III sources: two gallium cells, two aluminum cells, and an indium cell. The two gallium and two aluminum cells allow multiple AlGaAs compositions and growth rates without time-consuming cell temperature changes and without resorting to superlattice approximations of random-alloy AlGaAs and the high number of shutter operations required to achieve them. Vertical Cavity Surface Emitting Lasers (VCSEL's) require very accurate knowledge of the material growth rates in the MBE system. To improve the reproducibility of the growths, extensive work has been carried out to determine the most precise and accurate procedures and conditions for Reflection High Energy Electron Diffraction (RHEED) oscillation growth rate measurements. This work has improved the accuracy of the RHEED oscillation measurements to within  $\pm 1\%$ . We have also determined conditions to allow accurate measurement of the growth rate of strained InGaAs on GaAs, to give better control of the indium content of the strained quantum well active region of the VCSEL structures. Most recently, an optical monitoring system has been developed that allows measurement of the optical characteristics of the VCSEL

structure at a midpoint in the growth to determine the actual thickness of the structure and to correct for error in the original growth rate measurement. This system involves white-light coupled to a fiber, reflected off the substrate while it is in the growth position in the MBE, collected back in the fiber, and analyzed by a Optical Spectrum Analyzer to give the reflectivity spectrum of the partially-grown device. This reflectivity is compared to calculated reflectivity spectra for the device at that stage of growth and the differences used to determine the actual growth rate of the device. The new growth rates and the optical measurement can then be used to determine the thickness of the cavity as grown and to finish the cavity growth so that the cavity mode is in the proper position. Using this measurement technique, the cavity resonance can be controlled to within 0.2%. This allows the VCSEL structures to be grown repeatably with tight control of the offset between the peak gain of the quantum wells and the lasing mode of the vertical cavity structure, an important parameter in determining the device's thermal characteristics.

### ***III. Vertical Cavity Surface Emitting Laser Research***

Beyond the improvements in the growth technology carried out to enhance the reproducibility of the VCSEL growth, several advances in the state of the art in VCSEL devices have been achieved under the ARO program[8, 9]. First are the advances predicted by device modeling in the early stages of the program. Modeling on the thermal behavior of our first VCSEL devices indicated that the major drawbacks in the epitaxial design were in two areas. The first was the cladding material making up the cavity of the VCSEL. This material was seen in modeling to be of too low aluminum content, and that consequently, as the device heated, much of the carrier concentration in the wells was spilling out into the cladding material and recombining nonradiatively. This caused the devices to shut off prematurely. The second major factor was the placement of the peak gain of the quantum wells. The etched-pillar device structure used in our devices exhibits significant heating at the active region during operation. Because the cavity modes are widely spaced (approximately 50 nm apart), the VCSEL does not lase at the peak of the quantum well gain as an in-plane laser does. The lasing mode and the gain peak are independently set during the growth. During operation, by the time the device reaches threshold current, the active region is significantly above room temperature. If the device is grown so that the gain peak and cavity mode line up at room temperature, they will not line up during operation and the threshold current is increased to pump the wells to the gain required to reach threshold at the cavity wavelength. Modeling indicated that to improve the lasers, the cladding material aluminum content should be increased to 50% and the gain be offset to shorter wavelengths by roughly 25 nm to achieve more stable and higher power operation. These enhancements were incorporated in a VCSEL growth and the resulting devices set world records for CW high temperature operation, temperature independent threshold current (as can be seen in Figure 1), and CW power output. For the 8  $\mu\text{m}$  diameter device seen in Figure 1, the threshold was 1.4 mA at RT, decreasing to 1.2 mA at 55°C before increasing again.



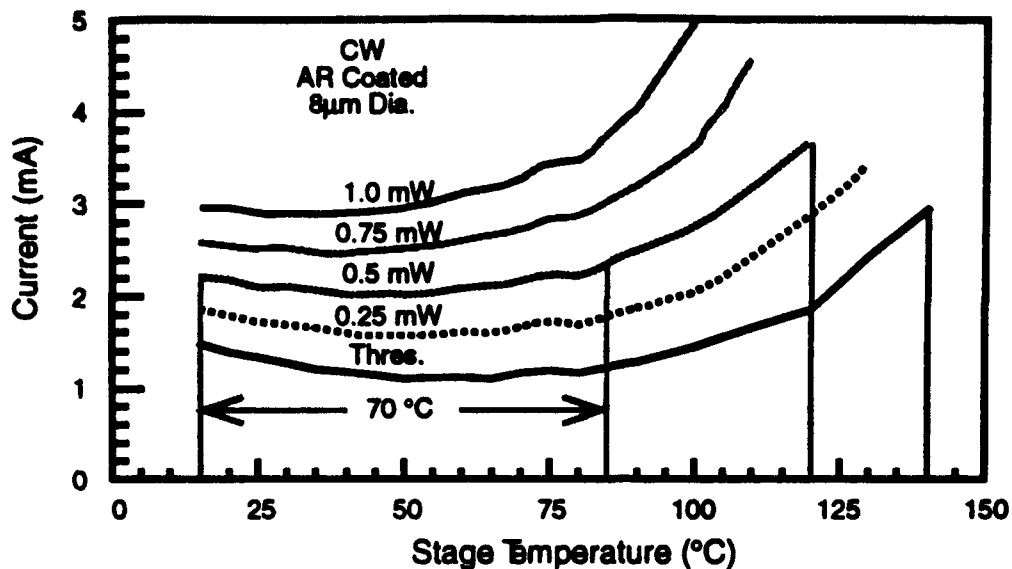


Figure 1. Current required to drive an 8μm diameter VCSEL to threshold and various power output levels as a function of temperature.

As can be seen in Figure 1, there is a 70°C range where the current required to achieve 0.5 mW output power varies by less than ±10%. A large diameter (70 μm) multimode device was heatsunk and the output power for the device increased to a record 114 mW CW.

More recently, work has been carried out on reducing the threshold current required to drive the VCSELs. An analysis of the current loss in small devices reveals that as the device diameter decreases, the current lost to surface recombination or carrier diffusion (if the quantum well is not etched through) becomes a dominant mechanism defining the device threshold current. Reduction or removal of this nonradiative carrier loss mechanism would result in a substantial reduction in threshold currents and a consequent improvement in power conversion efficiency as well as a reduction in the device heating for a given power output. To test this, VCSEL material similar to that described above was etched through the quantum wells by RIE and then passivated with various sulfide treatments prior to encapsulation with silicon nitride.

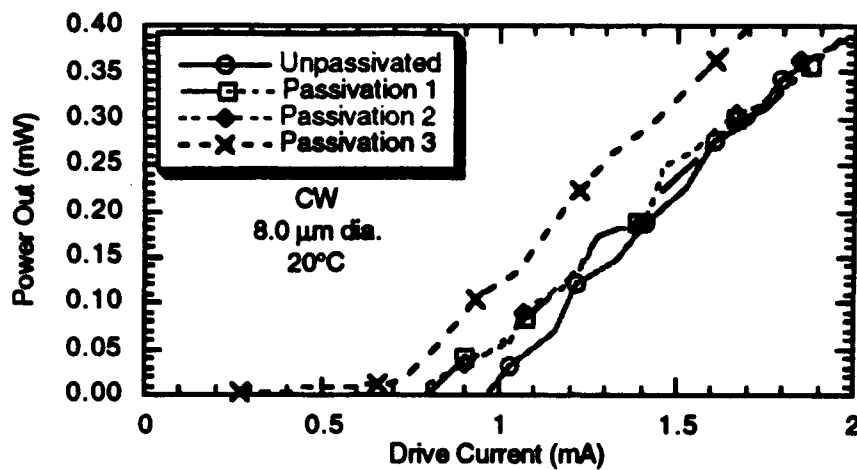


Figure 2. Light output vs. drive current for an 8  $\mu\text{m}$  diameter pillar with no passivation and with three different passivation techniques. The devices all reach a maximum of around 1 mW CW output power, but the figure has been blown up to show the reduction in threshold current for the passivated devices.

Figure 2 shows the threshold current of an 8  $\mu\text{m}$  diameter device with no passivation and three different passivation techniques. As can be seen, the threshold current for this device was reduced by approximately 33% over the untreated control device.

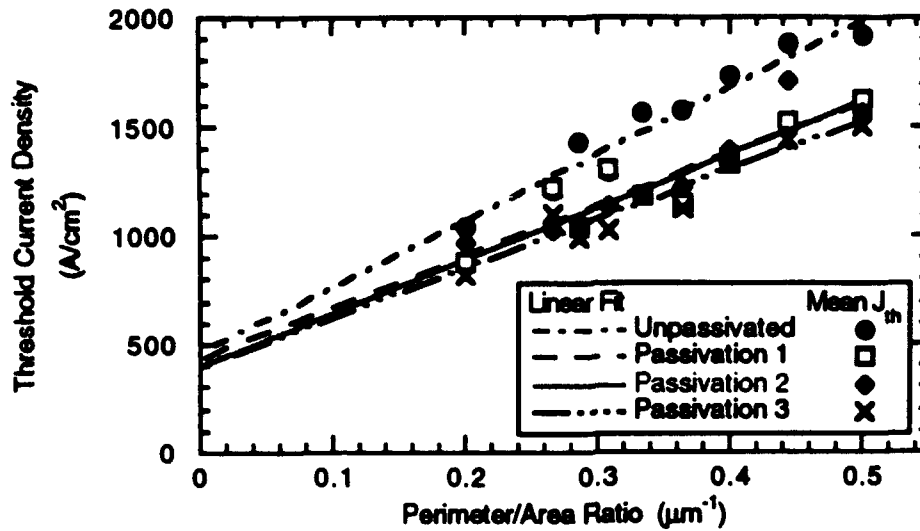


Figure 3. Threshold current density vs. the perimeter/area ratio of different diameter devices. A perimeter/area ratio of 0 corresponds to the broad-area device threshold current density, and a ratio of 0.5 corresponds to an  $8\mu\text{m}$  diameter VCSEL.

Figure 3 illustrates the increasing effect of surface recombination on the threshold current density of small VCSEL pillars. The slopes of the curves can be used to extract a surface recombination velocity, and a 25% reduction in surface recombination velocity was observed for the best passivation technique applied to these devices. This treatment resulted in a device with a record combination of low threshold (0.67 mA) and peak CW power output (1.2 mW). The results on the passivation are encouraging, but it is expected that with further refinements in the passivation, more significant reductions in the threshold current can be expected.

#### *IV. Modelling for reduced threshold VCSELs*

With the ability to accurately estimate the threshold current densities and differential efficiencies of broad area VCSELs, we feel confident about the theoretical models which have been developed to determine the gain as a function of current density as well as the various cavity losses, both mirror and free carrier absorption losses. Such knowledge has allowed us to optimize the design of VCSEL structures. We have for the most part settled on a three quantum well design with 1% transmission through the output coupler (which provides 99.5% mean mirror reflectivity). These numbers are based upon the internal losses of the cavity which we have attempted to minimize. Further reductions in the internal losses would allow us to reduce the transmission through the output coupler while keeping the differential efficiency constant, leading to lower threshold currents. However, while minimizing internal loss is an important aspect of the design, we have come to the conclusion that a better approach to minimizing the threshold current involves reducing the size of the VCSEL. Thus, this would appear to be a good direction in which to focus.

The challenge is to understand how the laser parameters are modified when the pillar diameter is made smaller than  $\approx 20\text{ }\mu\text{m}$ . We believe there are three main effects that must be dealt with: (1) surface recombination at the exposed sidewalls of the active region which increases the threshold current density, (2) optical scattering at the rough sidewalls of the pillar which increases the internal losses of the cavity, and (3) increased thermal impedance of the pillar which increases the temperature of the active region for a given power dissipation, ultimately limiting the maximum CW output power the device can produce. Surface recombination and the thermal impedance are expected to increase as  $1/r$ , where  $r$  is the radius of the pillar. Optical scattering on the other hand is expected to increase as  $1/r^3$ . The experimental dependence of the pulsed threshold current density on radius measured in our lab falls somewhere between  $1/r$  and  $1/r^3$  (for VCSELs greater than  $5\text{ }\mu\text{m}$ ), suggesting that both surface recombination and optical scattering are important. However, because the optical scattering has a much stronger dependence on  $r$ , it is our belief that the key to obtaining good

performance from VCSELs with diameters  $< 5 \mu\text{m}$  must include some method of reducing optical scattering.

Let us first consider surface recombination. Theoretical and experimental broad area VCSELs have threshold current densities in the range of  $600\text{-}1000 \text{ A/cm}^2$ , which in practical units is equivalent to  $0.6\text{-}1 \text{ mA}/(10\mu\text{m})^2$ . Thus,  $10 \mu\text{m}$  diameter pillars should have threshold currents  $< 1 \text{ mA}$ . Experimental  $10 \mu\text{m}$  diameter devices typically measure in at  $1.5\text{-}2 \text{ mA}$ . Using theoretical numbers for the threshold carrier density and surface recombination velocities typical of InGaAs/GaAs strained quantum wells, it is predicted that half of this threshold current is due to surface recombination. As the diameter is reduced, this fraction increases, thus representing a serious limitation on realizing small diameter VCSELs. In response to this difficulty, we have developed a number of methods to reduce the surface recombination. The surface passivation techniques were outlined above. Also, surface implantation techniques to disorder the quantum wells near the edge of the pillar as well as *in-situ* methods of regrowth to properly terminate the active region at the sidewalls of in-plane lasers are being explored. If successful, these techniques will eventually be applied to VCSELs.

As mentioned earlier, optical scattering also may represent a serious limitation due to its strong dependence on the device size. Unfortunately, quantitative theoretical estimates of the actual loss incurred from rough sidewalls is difficult to estimate. However, the relative dependence is easy to calculate if we assume that the loss is proportional to the power existing at the surfaces. Solving for the cylindrical Bessel function modes of the pillar has allowed us to observe how the losses should vary with radius. At small dimensions, it appears essential to attempt to suppress the fields at the surface. One method we are attempting to implement involves doping the sidewalls to reduce the index there as a result of the plasma effect. Even though these index changes are small, we have found that a  $0.5\%$  change in index penetrating  $0.5 \mu\text{m}$  into the  $6 \mu\text{m}$  diameter pillar is enough to significantly suppress the power at the surface. Such numbers are attainable using sidewall implantation or diffusion. One other concern was that the doping in the sidewalls would actually introduce more internal loss. Our calculations

reveal that the confinement factor in the lossy areas decreases more rapidly than the losses increase, as the index is changed (assuming free carrier absorption loss increases linearly with carrier density). As a result, the higher the doping, the better is the loss. Furthermore, the expected modal losses for moderate doping is expected to be  $< 0.02\%$ , a factor of ten smaller than other losses in the cavity. Thus, we are very optimistic about reducing optical scattering losses.

The final concern with small diameter VCSELs involves the thermal impedance. With the  $1/r$  dependence, we anticipate heating to be a major problem. The most direct way to combat this problem is to heat sink the devices either by flip-chip bonding or by creating trenches around the VCSEL which can then be filled with a good thermal conductor. We are currently working on developing the technology necessary to implement such low thermal impedance devices.

We anticipate that with the above solutions to small VCSEL device problems, the threshold currents can be reduced close to the broad area device limit. For example, using the  $1 \text{ mA}/(10\mu\text{m})^2$  threshold current density measured in broad area devices, a  $5 \mu\text{m}$  diameter device should have less than  $0.25 \text{ mA}$  threshold current. However, we anticipate that devices as small as  $2\text{-}3 \mu\text{m}$  in diameter should be attainable. Thus, we expect threshold currents to eventually drop below  $100 \mu\text{A}$ , while simultaneously maintaining reasonable differential efficiencies. And with good heat sinking, CW powers greater than  $1 \text{ mW}$  should also be possible in such devices.

## V. Quantum-wire lasers and Characterization

In the quantum wire laser area, a key effort provided optical gain measurements from a serpentine superlattice nanowire array laser sample grown by MBE on a 2°-off (100) GaAs vicinal substrate[\*\*15]. The sample was fabricated into in-plane ridge-waveguide lasers with stripes either parallel or perpendicular to the nanowire arrays. Spontaneous emission spectra were taken at 1.4 K and 77 K for several injection levels. The measured gain spectra at 1.4 K show extraordinary anisotropic characteristics. It is demonstrated that TM mode gain becomes greater than TE mode gain when the optical cavity is placed along the nanowire direction which gives strong evidence that the lateral quantum confinement in the serpentine superlattice is stronger than the vertical quantum confinement. A novel theoretical model has been proposed and applied to the calculation of optical gain spectra in the serpentine superlattice with consideration of both homogeneous and inhomogeneous broadening[4]. The observed polarization-dependent gain spectra are well-explained by this model. A good fit to the data is achieved when the lineshape functions are assumed to have Gaussian distribution with FWHM energy of 6 meV for the homogeneous broadening and 15 meV for the inhomogeneous broadening.

In order to generate the above described data, a self-consistent method for measuring the material gain/current-density characteristics in ridge lasers was developed[\*14]. Ridge waveguide lasers were made, with different stripe widths and ridge heights, by *in situ* laser-monitored reactive ion etching. The leakage current, consisting of mainly ohmic-sheet spreading current and lateral diffusion current, is determined from the variation of threshold current versus stripe width and cavity length. It is found that the inclusion of leakage current is crucial to obtain a self-consistent result. By using this method, the gain/current-density curve for a 8 nm-wide  $\text{In}_{0.2}\text{Ga}_{0.8}\text{As}/\text{AlGaAs}$  strained single-quantum-well laser sample is measured to have a transparency current density of 45.4 A/cm<sup>2</sup>.

## ***VI. In-situ etching and regrowth***

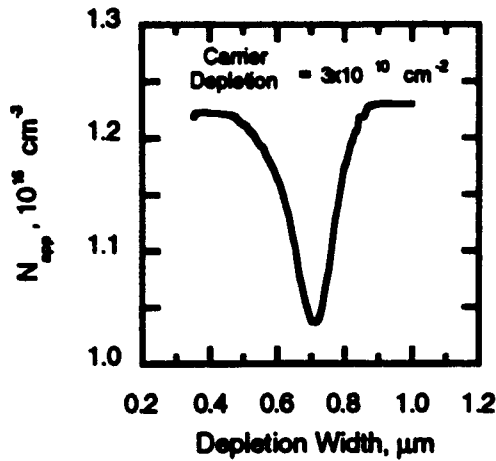
We have installed an etching/analysis chamber and connected it with two MBE chambers to make an UHV in-situ processing system[16]. The etching capabilities include a broad-area ion beam source and a reactive gas inlet with microwave cracking capability. This allows us to do both low-damage thermal gas etching and anisotropic ion-beam assisted etching. The system base pressure is  $5 \times 10^{-8}$  Torr, with oxygen and water partial pressures at  $2 \times 10^{-10}$  and  $4 \times 10^{-11}$  Torr, respectively. These low partial pressures make possible the smooth etching of aluminum-containing materials.

Analytical tools include a focused electron beam and secondary electron detector which give us an electron microscope inside the etch chamber and the possibility of in-situ patterning, and an attached RHEED system which allows us to investigate the etched surface roughness. We use laser reflectance to monitor the progression of an etch in real time.

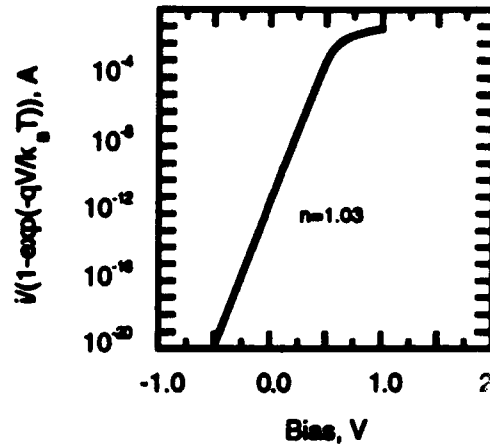
### **1. Electrical quality of regrowth interface:**

We have used in-situ etch and regrowth to achieve interface trap densities as low as  $10^{10}$   $\text{cm}^{-2}$  with gas etching. We have fabricated Schottky diodes on regrown GaAs which display ideal I-V characteristics and no observable current-limiting effect by the regrowth interface. In view of these promising results, we are applying this etch-and-regrowth technique to the fabrication of gain-coupled DFB and buried in-plane lasers.





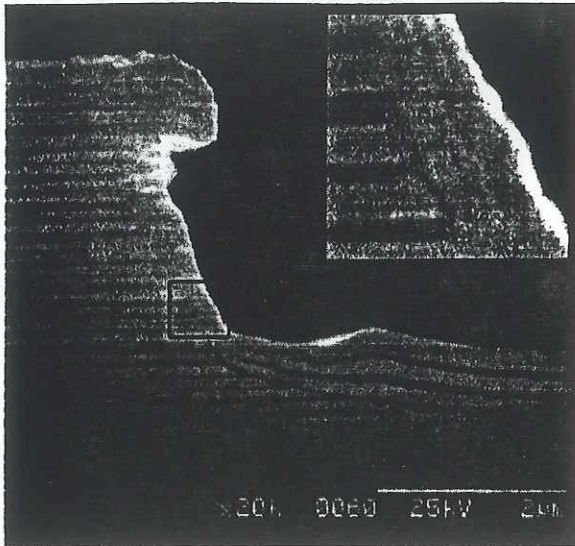
CV Profile of Chemical  
Gas Etched Interface



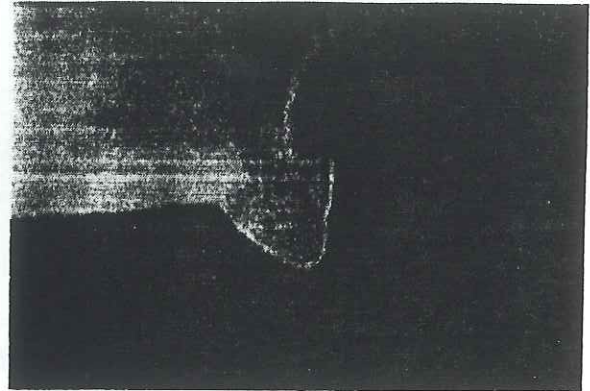
Schottky Plot Showing  
Ideality of the Diode

## 2. Regrowth over etched structures:

We have demonstrated in-situ regrowth of GaAs and AlAs layers over etched GaAs and AlAs structures. SEM pictures show that the epilayers adhere to the etched sidewalls – an important result for making buried in-plane lasers with low surface recombination currents. Using SiO<sub>2</sub> as an etch mask, we have also demonstrated liftoff of polycrystalline layers deposited on the mask during regrowth, leaving the original device surface unharmed.



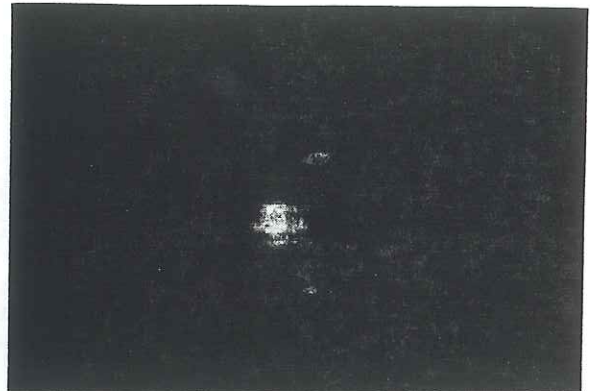
SEM micrograph of GaAs (light) and AlAs (dark) regrowth layers over etched GaAs/AlAs mirror stack. (Uneven layers due to excessive stain etching). Inset shows regrowth on sidewall. Etched with IBAE followed by gas etching.



GaAs and AlAs epilayers deposited on a  $\text{SiO}_2$  etch mask (top) and their removal by HF liftoff (bottom).

### 3. Surface morphology:

We have demonstrated smooth Ion Beam Assisted Etching (IBAE) and thermal gas (chlorine) etching of  $\text{Al}_x\text{Ga}_{1-x}\text{As}$ ,  $\text{In}_{0.53}\text{Ga}_{0.47}\text{As}$ , and  $\text{InP}$ , as measured with Nomarski microscopy. In addition, we have studied the atomic-scale surface of etched GaAs with RHEED and atomic force microscopy. Chlorine gas etching at  $200^\circ\text{C}$  results in a surface roughness on the order of  $100\text{\AA}$ .



RHEED pattern after 200°C chlorine gas etching (left) and after 90Å growth of GaAs (right). Faceting is evident on the etched surface (chevron-shaped diffraction streaks). Regrowth smooths the surface as evidenced by the streaky pattern.

#### 4. Buried in-plane lasers:

Using the etch and regrowth techniques discussed above we have fabricated buried in-plane lasers. The reduction in surface recombination achieved by regrowth of material on the edges of the active region results in reduced threshold current: in a 5  $\mu\text{m}$ -wide laser stripe the threshold current density was cut in half, due to the reduction in surface recombination velocity (S) from  $2 \times 10^5$  cm/s to  $9 \times 10^4$  cm/s. Further improvements are expected, as indicated by the electrical results discussed above.

## **VII. Participating Scientific Personnel**

L.A. Coldren	Principal Investigator
A.C. Gossard	Co-Principal Investigator
J.H. English	Development Engineer
D. Mui	Post Doc
S.W. Corzine, S.Y. Hu, D.B. Young, T. Strand, R. Herrick, S.-L. Lee	Students

**VIII. Appendix I - Summary Foils from Technology Transfer workshop, Los Angeles, 2/3/93.**

**Presenter:** Larry A. Coldren

**Organization:** University of California, Santa Barbara

**Title:** Materials and Processing Technologies for Quantum Confined Optoelectronic Device Structures

**Summary:**

The technology to grow and process optoelectronic materials for high efficiency devices has been advanced under this IST/SDIO program. Novel ultra-high vacuum *in situ* processing apparatus has been developed which contains chambers for the epitaxial growth of 'quantum-confined' device structures as well as their lateral patterning by low-damage etching. Using this apparatus, novel optoelectronic structures have been fabricated. The one with the most immediate commercial potential is a vertical-cavity surface-emitting laser. Advanced design and analysis software has also been developed for this and other related semiconductor lasers under the SDI program. This device technology and design expertise is being transferred to several companies. Patents have been granted on the low-damage etching apparatus, the processing recipe and some device embodiments.

# **Materials and Processing Technologies for Quantum-Confined Optoelectronic Device Structures**

by

**Larry A. Coldren**  
University of California, Santa Barbara, CA

February 3, 1993

Sponsored by IST/SDIO via ARO

## **Introduction**

- **UCSB has one of the largest university efforts in III-V semiconductor technology**

- A dozen leading faculty involved in all aspects
- State-of-the-art growth and processing facilities
  - 5 MBEs; *in-situ* etching/growth; FIB; Liquid MOCVD; E-beam; Clean room
- State-of-the-art characterization facilities
- An NSF sponsored Science and Technology Center on Quantum-Confined Electronic Structures (QUEST), an NSF-Materials Research Lab, and a DARPA/industry sponsored Optoelectronics Technology Center (OTC)

- **IST/SDIO instrumental in setting up and supporting growth and processing facilities as well as device and modelling work**

- Integrated UHV system: MBE + *in-situ* etching by SDIO; a second MBE and FIB from other sources.
- Novel radical-beam ion-beam etching (RBIBE) technique\* installed *in-situ*
- Support of advanced software development for MBE control\*\* as well as optoelectronic device modelling\*\*
- Early support of leading tunable\* and vertical-cavity\* laser work

\*Patented;

\*\*copyrighted

# SPONTANEOUS EMISSION FACTOR

IEEE JOURNAL OF QUANTUM ELECTRONICS, VOL. 24, NO. 5, MAY 1988

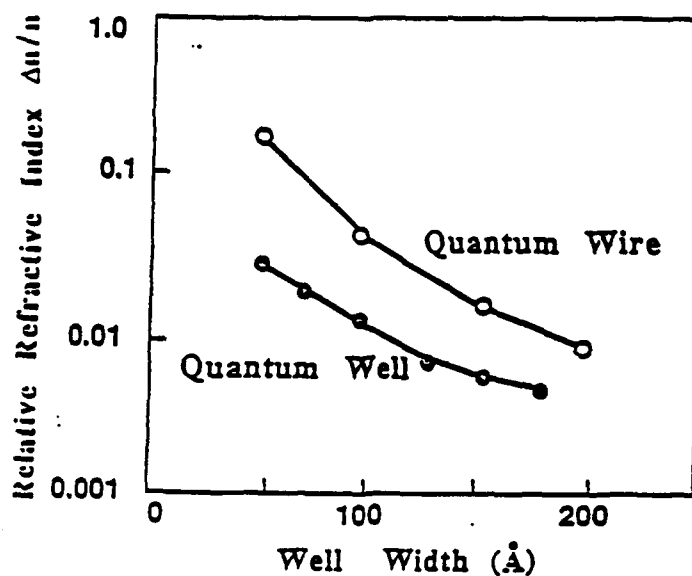
TABLE I  
QUANTUM EFFECTS AND PROPERTIES OF  $\beta$  FACTOR FOR EACH  
ACTIVE REGION

Active Region	Bulk	QF		QW		QB
		$r = \infty$	$r = 1$	$r = 0.3$		
$\xi, m$	1	2	2	2		2
$p$	1	1.5	1.1	0.81		0.75 - 1.5
$\Delta\lambda$ (nm)	0.5	0.5	0.67	0.91		> 0.5
$\Delta\lambda$ (nm)	30	15	5	5		< 1
$C/C_{max}$	1	6	18	18		> 50
$C_{max}$	0.5	0.5	0.67	0.91		> 0.5

$\beta = \frac{\Delta\lambda}{\Delta\lambda_0}$

Relative Refractive Index  $\Delta n/n$  AT PEAK

QUANTUM-WIRE vs QUANTUM-WELL  
(THEORY)





## Technology Description

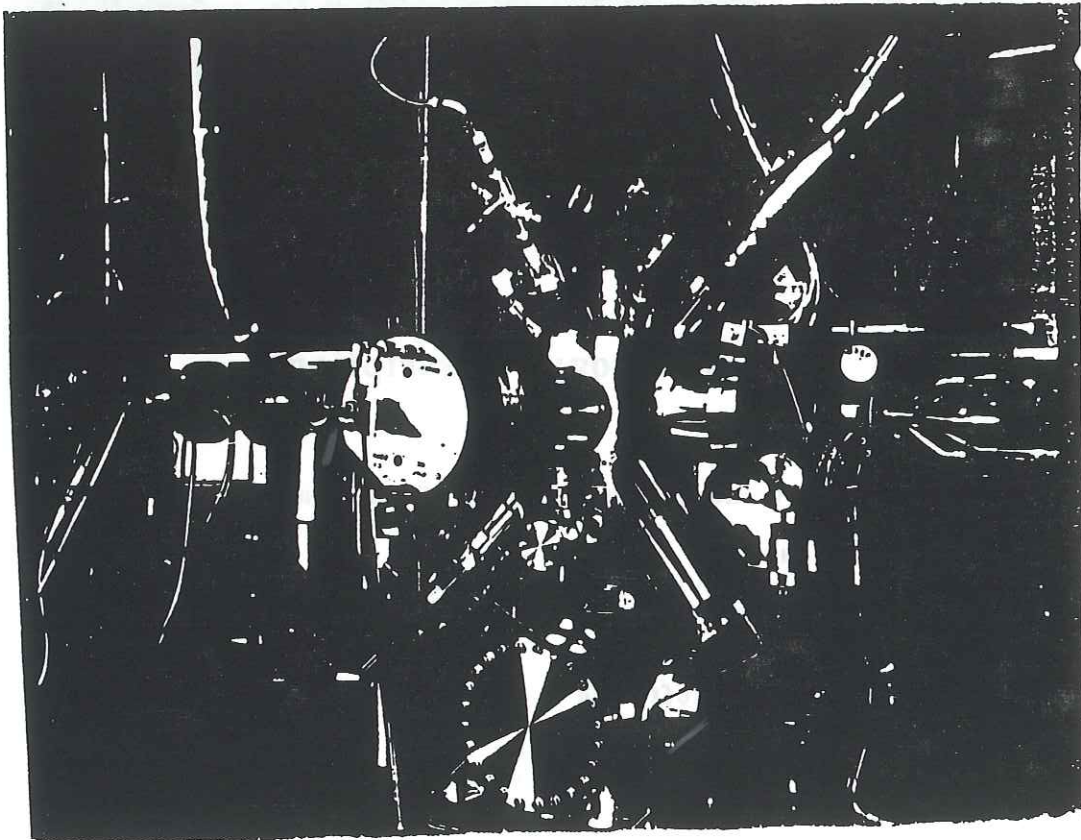
- **Novel low-damage, anisotropic etching apparatus and technique**
  - RBIBE: #4,874,459
  - Incorporation into UHV in-situ processing apparatus: model for integrated growth & processing factory
- **User-friendly software**
  - MBE control: MBE-MASTER
    - Transferred to Sandia, Xerox, yyy, zzz
  - Analysis and design of vertical-cavity lasers: MULTILAYER; GAIN; VCSEL
    - Transferred to Honeywell, AT&T, Hewlett-Packard
- **Novel optoelectronic devices**
  - Ultra-wide tuning range laser: #4,896,325
  - Efficient vertical-cavity laser: #4,873,696



## Innovative Elements--1

- RBIBE

- Only technique to cover full range from purely physical to purely chemical dry etching
- Physical etching is independently controlled from the chemical and the chemical effect is stronger
- Anisotropy can be achieved with minimum damage
- Etch rate can be maximized with minimum damage and controlled anisotropy (record reactive sputter yield)
- Desired for many device applications where high-aspect features are needed



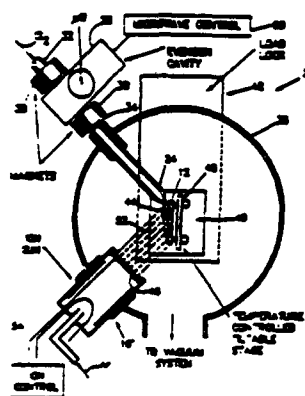
## Goldman et al.

(45) Date of Payment Oct. 17, 1960

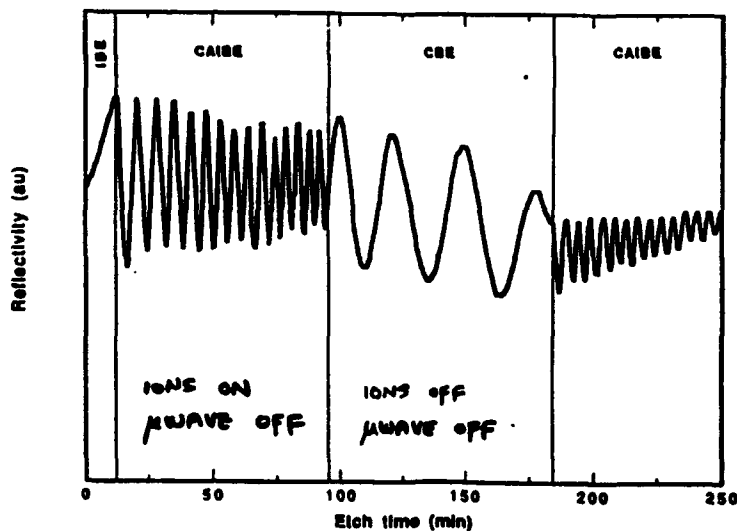
DATE 1/28/02 BY SP-4/2002

[illegible]

#### 40. Chlorine, 4 Densities Shown



### Reflectance of GaAs/AlAs Stack



## Innovative Elements--2

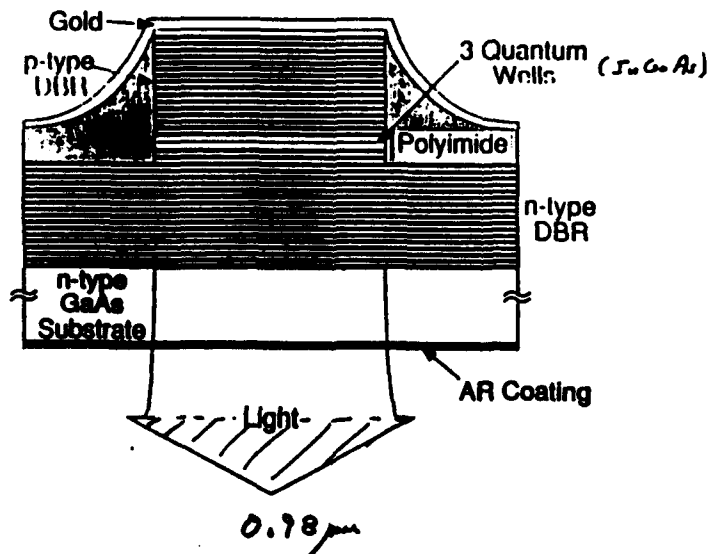
### • MBE Software

- Most user-friendly and versatile MBE control software available
- Many subprograms for exotic structures
- Communicate in high-level language: thickness and composition not machine settings.
- Improves output of MBE in quality and quantity

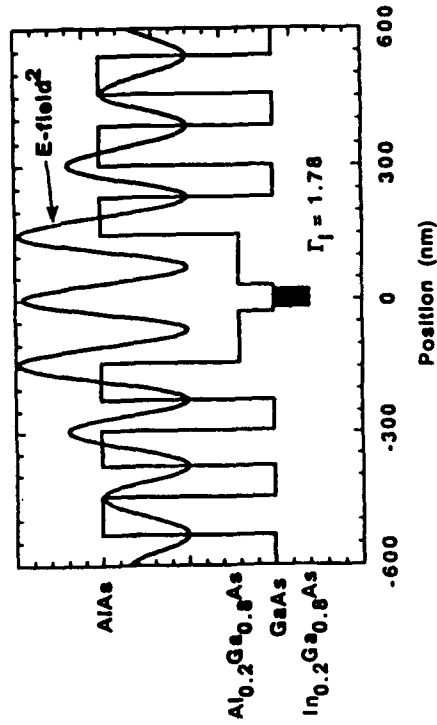
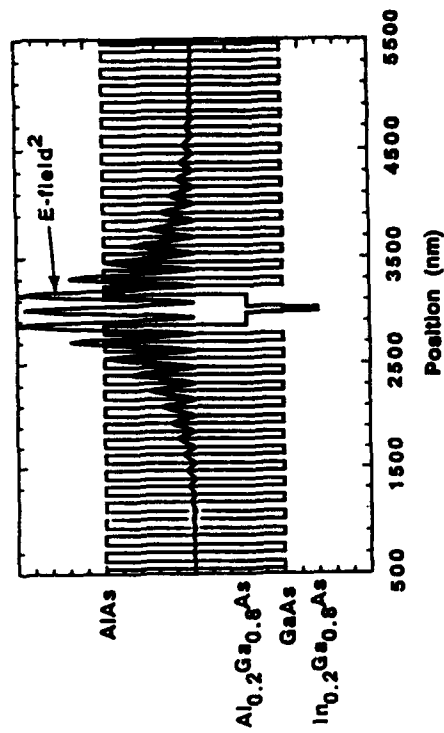
### • Device Analysis & Design Software

- Very efficient and user-friendly--Macintosh based
- Gain calculations done two-orders of magnitude more efficiently than other available programs
- VCSEL designs with minimal input
- Multilayer waveguide and standing-wave analysis
- Desirable for production of optimized devices

### VERTICAL-CAVITY SURFACE-EMITTING LASERS (VCSELs)



## Standard VCSEL Structure

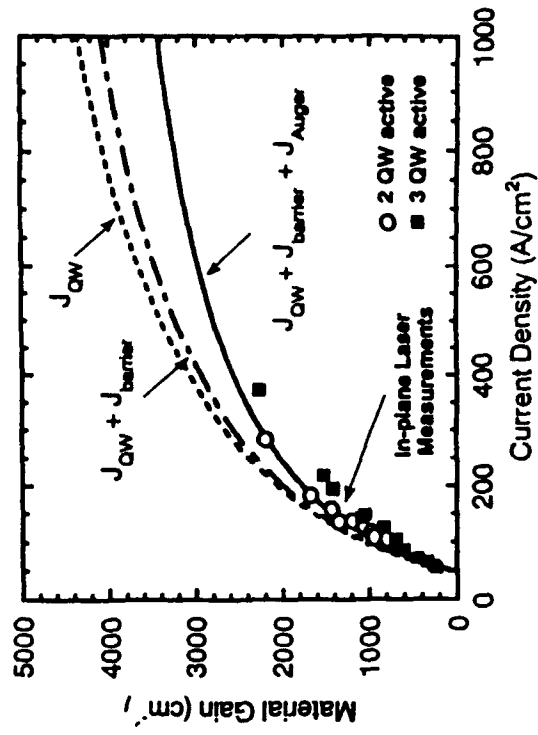


## Optical Gain in Strained and Unstrained Quantum Wells

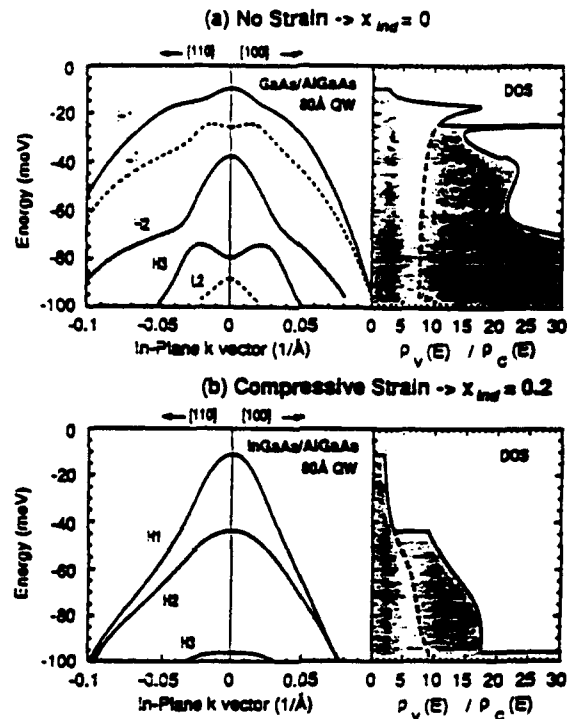
S.W. Corzine, B. Thibault, R.S. Geels, C.P. Chao,  
Radha Nagarajan, and L.A. Coldren

Sponsored by ARO

A detailed theoretical model of gain has been developed to predict effects of strain in both InGaAs/GaAs and InGaAs/InP material systems



## Valence Subband Structure (InGaAs/GaAs System)



Comparison of the valence subbands with and without strain. The density of states shown at the right indicates the much improved matching between the conduction and valence band in the strained case. (Ideally the ratio should be equal to 1).

## Innovative Elements--3

### • Novel Optoelectronic Devices

#### - Sampled-grating tunable diode laser

- Unsurpassed in tuning range ( $>60\text{nm}$ )
- Best combination of wide tuning range with good mode suppression
- Fabrication no more difficult than standard DBR laser--much simpler

than competition

- Needed in high-capacity wavelength division communication systems
- Ready for final development and manufacture

#### - Vertical-cavity laser

- Gain placement at standing-wave maximum doubles the modal gain
- High-bandgap confining layers and displaced gain design allows operation at high temperatures
- Temperature insensitive operation also demonstrated.
- Wafer-scale fabrication and testing provides first laser manufacturable

by IC technology

- Needed for numerous applications from data links to optical recording
- Ready for final development and manufacture

**[54] SURFACE-EMITTING LASERS WITH PERIODIC GAIN AND A PARALLEL DRIVEN NIP STRUCTURE****[72] Inventors:** Larry A. Coldren, Santa Barbara; Jeffrey W. Scott, and Victor Rios M. Yeh, Santa Barbara, Calif.**[73] Assignee:** The Regents of the University of California, Berkeley, Calif.**[21] App. No.:** 568,146**[22] Filed:** Oct. 27, 1988**[31] Int. Cl.:** H01S 3/39**[32] U.S. Cl.:** 372/96, 372/46**[38] Field of Search:** 372/96, 108, 44, 45, 372/46, 72**[56] References Cited****U.S. PATENT DOCUMENTS**

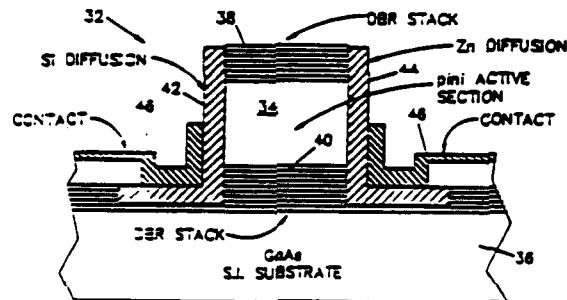
4,664,323	5/1987	Van Royen et al.	372/46
4,664,327	6/1987	Scott	372/46
4,664,328	5/1987	Adams et al.	372/96
4,673,376	6/1987	Scott	372/96
4,768,101	11/1987	Neumann et al.	372/46
4,732,934	6/1988	Neumann et al.	372/46
4,797,880	1/1989	Scott et al.	372/46

Primary Examiner—James W. Davis  
 Attorney, Agent, or Firm—Donald A. Serock

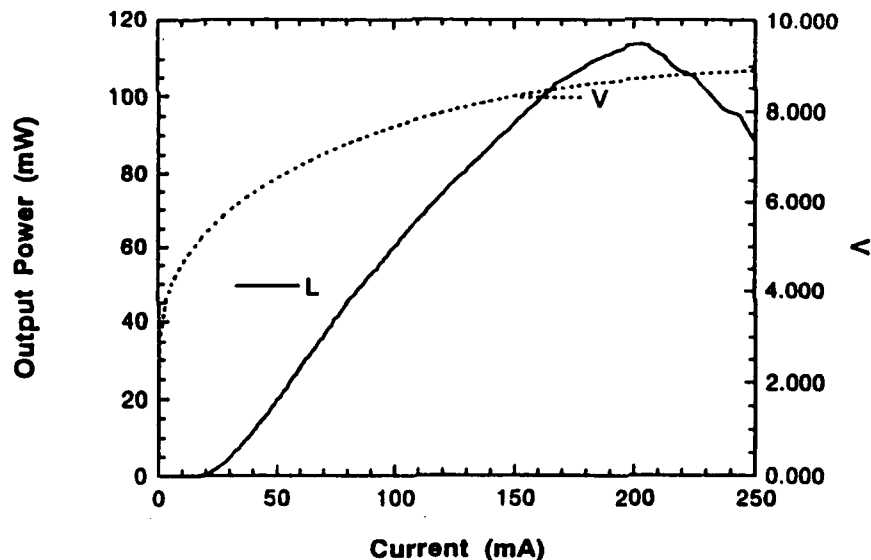
**[57] ABSTRACT**

A surface-normal cavity, AlGaAs Distributed-Brugg Reflectors laser. The laser is constructed on a GaAs substrate. There is a separate gain-producing active section composed of a plurality of gain-producing regions disposed at periodic intervals with respect to the wavelength of an intended operating frequency of the laser is located vertically with respect to the surface of the substrate. A pair of Distributed-Brugg-Reflectors are disposed at the respective ends of the separate active section. A pair of electrodes are formed on either side of and operatively connected to the separate active section in electrical contact therewith for applying a driving current to the separate active section in parallel. In one embodiment, the separate active section has interfaces between p- and n- regions formed by alternating wave sections of the intended operating frequency of the laser. In another, the separate active section has interfaces between p- and n- regions formed by alternating wave sections of the intended operating frequency of the laser in amount which will allow the impedance discontinuity of the wave segment to result in more in-phase reflection components whereby the gain-producing active section acts as a mirror and the net reflective reflectivity of the laser is increased.

19 Claims, 3 Drawing Sheets

**DIAMOND HEATSINK**

CW Output Power for  
 70  $\mu\text{m}$  diameter device



As the light of December 29, 1932, dawned on France, the French people were still in the grip of the depression. The unemployment rate was 20 per cent, and the government was in a desperate straits. The French people were in a state of despair, and the government was in a state of panic. The French people were in a state of despair, and the government was in a state of panic. The French people were in a state of despair, and the government was in a state of panic.

[illegible]

(194) MULTI-SECTION TUNABLE LASER WITH  
CONTINUOUS MULTI-ELEMENT MODES

(195) Inventor: Larry A. Colburn, Santa Barbara,  
Calif.

(17) **Augustus** The Regents of the University of California, Berkeley, Calif.

[illegible]

154	_____	372/102	372/11	372/29
155	Field of Stone	_____	372/104	372/31
156	_____	372/102	372/102	372/32

196  
Reference Code  
U.S. PATENT DOCUMENTS  
JUL 11 1966 2:45 PM  
174

OTHER PUBLICATIONS

Primary Emotions—John Sarno, Jr.  
 Research About the Human Mind—A. Sarno

100-443887-100  
DECLASSIFIED  
DATE 03-01-2001

\_\_\_\_\_

48-

VENUE

CONTINUED

44 CASH CONTROL

8-	
8-	

	MIRROR	GAIN
1	0.0000	0.0000
2	0.0000	0.0000
3	0.0000	0.0000
4	0.0000	0.0000
5	0.0000	0.0000
6	0.0000	0.0000
7	0.0000	0.0000
8	0.0000	0.0000
9	0.0000	0.0000
10	0.0000	0.0000
11	0.0000	0.0000
12	0.0000	0.0000
13	0.0000	0.0000
14	0.0000	0.0000
15	0.0000	0.0000
16	0.0000	0.0000
17	0.0000	0.0000
18	0.0000	0.0000
19	0.0000	0.0000
20	0.0000	0.0000
21	0.0000	0.0000
22	0.0000	0.0000
23	0.0000	0.0000
24	0.0000	0.0000
25	0.0000	0.0000
26	0.0000	0.0000
27	0.0000	0.0000
28	0.0000	0.0000
29	0.0000	0.0000
30	0.0000	0.0000
31	0.0000	0.0000
32	0.0000	0.0000
33	0.0000	0.0000
34	0.0000	0.0000
35	0.0000	0.0000
36	0.0000	0.0000
37	0.0000	0.0000
38	0.0000	0.0000
39	0.0000	0.0000
40	0.0000	0.0000
41	0.0000	0.0000
42	0.0000	0.0000
43	0.0000	0.0000
44	0.0000	0.0000
45	0.0000	0.0000
46	0.0000	0.0000
47	0.0000	0.0000
48	0.0000	0.0000
49	0.0000	0.0000
50	0.0000	0.0000
51	0.0000	0.0000
52	0.0000	0.0000
53	0.0000	0.0000
54	0.0000	0.0000
55	0.0000	0.0000
56	0.0000	0.0000
57	0.0000	0.0000
58	0.0000	0.0000
59	0.0000	0.0000
60	0.0000	0.0000
61	0.0000	0.0000
62	0.0000	0.0000
63	0.0000	0.0000
64	0.0000	0.0000
65	0.0000	0.0000
66	0.0000	0.0000
67	0.0000	0.0000
68	0.0000	0.0000
69	0.0000	0.0000
70	0.0000	0.0000
71	0.0000	0.0000
72	0.0000	0.0000
73	0.0000	0.0000
74	0.0000	0.0000
75	0.0000	0.0000
76	0.0000	0.0000
77	0.0000	0.0000
78	0.0000	0.0000
79	0.0000	0.0000
80	0.0000	0.0000
81	0.0000	0.0000
82	0.0000	0.0000
83	0.0000	0.0000
84	0.0000	0.0000
85	0.0000	0.0000
86	0.0000	0.0000
87	0.0000	0.0000
88	0.0000	0.0000
89	0.0000	0.0000
90	0.0000	0.0000
91	0.0000	0.0000
92	0.0000	0.0000
93	0.0000	0.0000
94	0.0000	0.0000
95	0.0000	0.0000
96	0.0000	0.0000
97	0.0000	0.0000
98	0.0000	0.0000
99	0.0000	0.0000
100	0.0000	0.0000

---

1

\_\_\_\_\_

## Wallplug Efficiencies of VCSELs with $\text{Al}_{0.7}\text{Ga}_{0.3}\text{As}/\text{GaAs}$ p-type DBR mirror.

20 Peak = 14.9%

30



DIA=40nm

10

\_\_\_\_\_

7

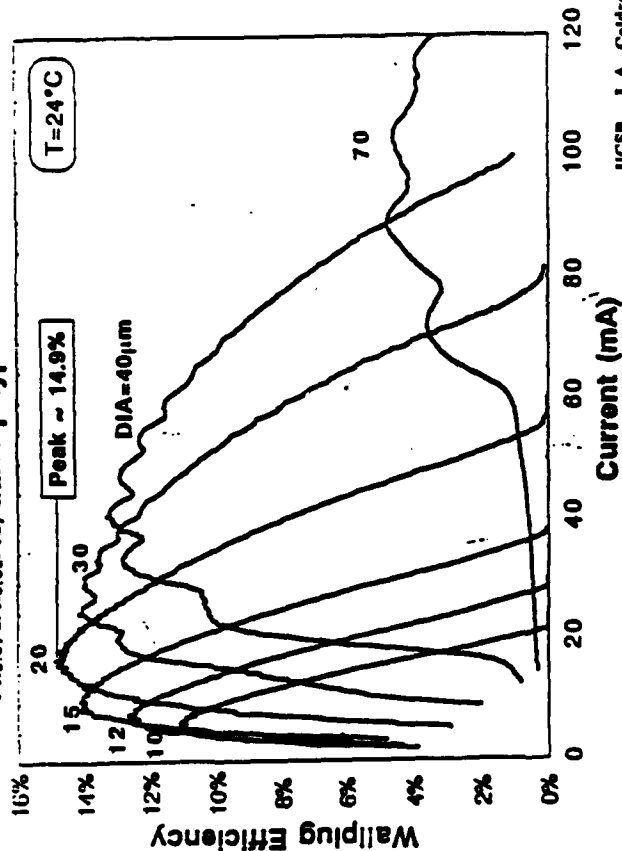
\_\_\_\_\_

1	2	3	4	5	6	7	8	9	10	11	12	13	14	15	16	17	18	19	20	21	22	23	24	25	26	27	28	29	30	31	32	33	34	35	36	37	38	39	40	41	42	43	44	45	46	47	48	49	50	51	52	53	54	55	56	57	58	59	60	61	62	63	64	65	66	67	68	69	70	71	72	73	74	75	76	77	78	79	80	81	82	83	84	85	86	87	88	89	90	91	92	93	94	95	96	97	98	99	100
---	---	---	---	---	---	---	---	---	----	----	----	----	----	----	----	----	----	----	----	----	----	----	----	----	----	----	----	----	----	----	----	----	----	----	----	----	----	----	----	----	----	----	----	----	----	----	----	----	----	----	----	----	----	----	----	----	----	----	----	----	----	----	----	----	----	----	----	----	----	----	----	----	----	----	----	----	----	----	----	----	----	----	----	----	----	----	----	----	----	----	----	----	----	----	----	----	----	----	-----

Current (mA)

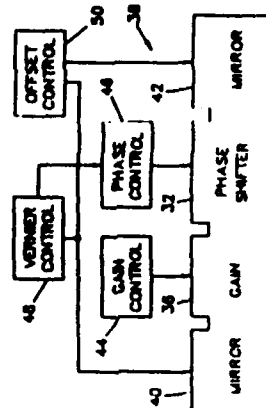
1997

0111



Now. 1970

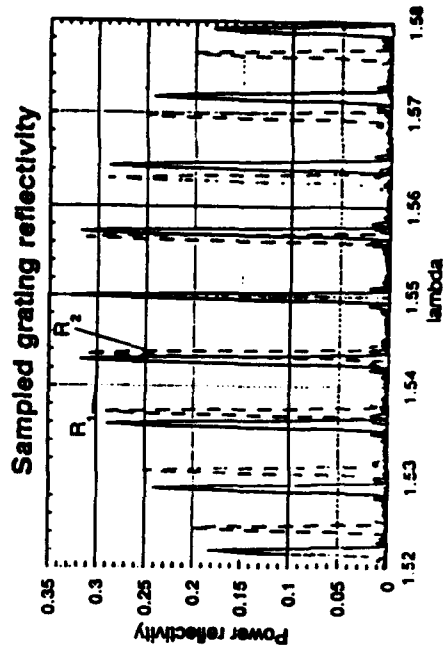
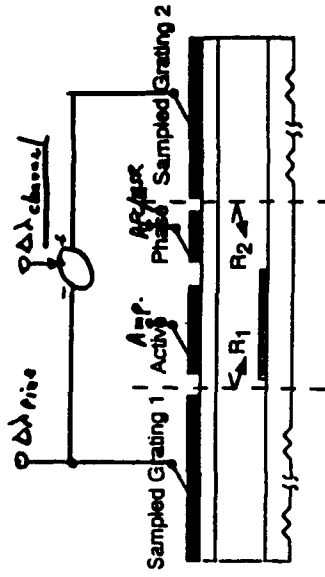
UCSB, L.A. Colding et al.  
submitted to Ekc. Lett.



上海各界救國委員會

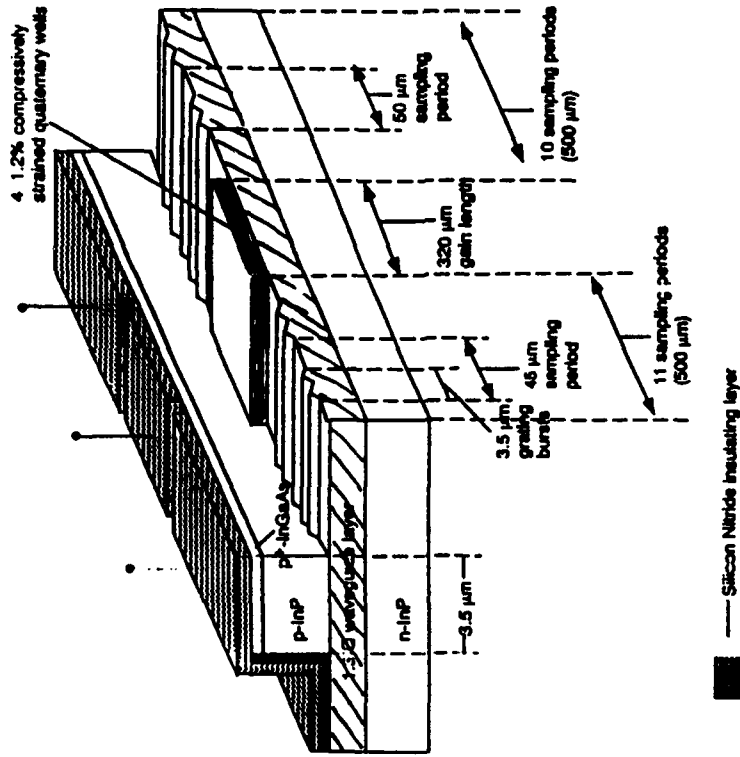
# Introduction: the sampled grating concept; proposed LEOS '91

Gratings with elements periodically removed lead to periodic reflection spectra and wideband "vernier scale" tuning.



$$\begin{aligned} \cdot (\Delta\lambda)_{\text{zero}} &\sim 57 \text{ nm} \\ \cdot (\Delta\lambda)_{\text{100-nm}} &\sim 7 \text{ nm} \\ \cdot (\Delta\lambda)_{\text{max}} &\sim 0.5 \text{ nm} \end{aligned}$$

## Device structure used in present work



— Silicon Nitride Insulating layer

— Ti:Ti/Au metallization

1. GROW THROUGH ACTIVE

2. REMOVE ACTIVE FROM GRATING

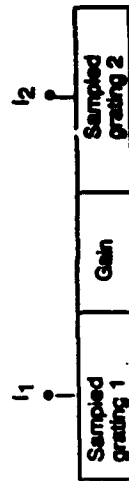
3. REGROW

4. RIDGE FORMERS



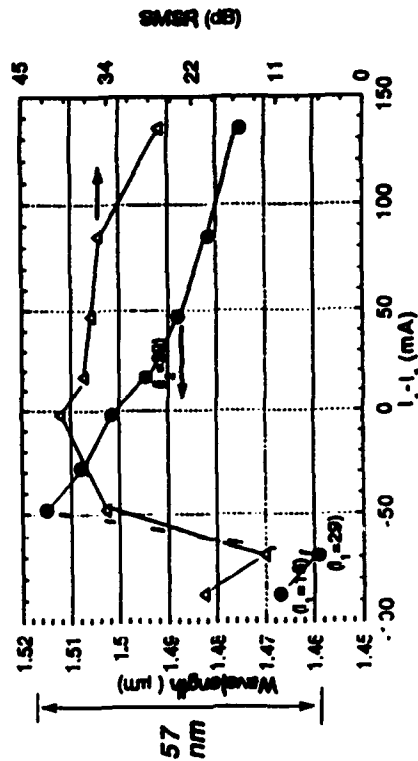
## Device Tuning Characteristics

- Tuning by primarily changing one mirror current, with occasional small adjustments in the other mirror current to maximize SMSR.
- SMSR maintained over 30 dB for most of tuning range.



• 64W Peak Too Low

### SGDBR tuning vs. difference in mirror currents

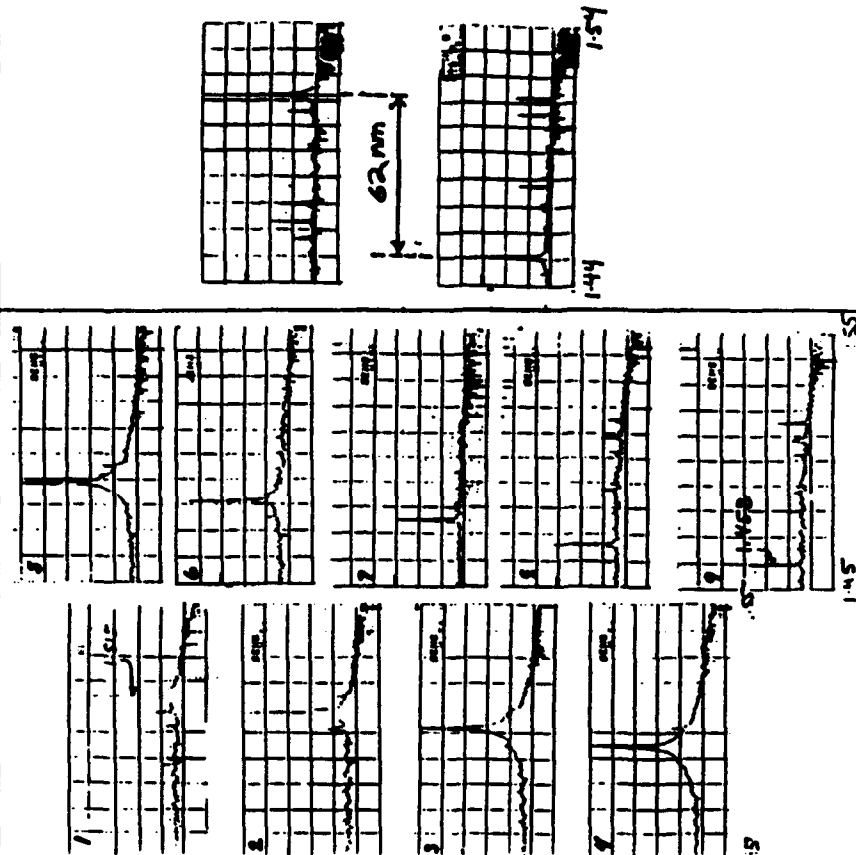


$$I_m \sim 30-40 \text{ mA}$$

## Time-averaged optical spectra under pulsed operation

(10 dB/vertical division and 100 nm full scale)

- 57 nm device
- 62 nm device with lower SMSR



• Output consistency over 3000

## **Future Developments**

- **Basic Technology available for licensing**
- **Although leading the pack, there are still many improvements possible in the tunable laser and vertical-cavity laser devices**
  - Ready for industrial development
  - Funding required

## **Spinoff Applications**

- **RBIBE**
  - Applicable to all manner of semiconductor component manufacture--not limited to III-Vs and certainly not only to military applications
  - Payoff because of improved control and speed
- **Software**
  - MBE control software useful in any MBE application
  - Gain analysis software useful for any diode laser
  - VCSEL analysis and design useful for many classes of VCSELs--applications not limited
  - Immediate payoff in growth quality and quantity and design savings
- **Devices**
  - Tunable lasers desired for wavelength division communication; spectroscopy; beam sweeping; holographic optical memory; and display--not limited to military applications
  - VCSELs superior to conventional in-plane lasers for most applications: printing; data links; high-frequency modulation; optical storage; display--not limited to military applications.
  - Ready for commercial development--demand is there for cost-effective devices

## **Key Players**

- The RBIBE technology is being emulated without licensing in many laboratories. Equipment manufacturers have expressed interest, but not takers yet.
- Hewlet-Packard, Honeywell, and Optical Concepts, Inc are developing the VCSEL technology with us. Others have expressed interest.
- Mild interest, but no firm takers for the tunable laser concepts. Our concept looks like a winner, but the market needs to develop.
- The software is being licensed or shared freely.
- The Japanese and Europeans will have competing activities.

## **Moving Forward**

- Small/large companies need incentives to develop these new technologies. R & D capital scarce.
- UCSB needs additional \$ from government sources to continue research, but more \$ should come via industries to provide for technology transfer.
- Companies need incentives to send employees on-campus to acquire new technological advances

## **IX. Appendix II - Publications resulting from ARO work**

1. Corzine and L.A. Coldren, "Theoretical gain in Compressive and Tensile Strained InGaAs/InGaAsP Quantum Wells," *Appl. Phys. Lett.*, **59**, (5), 588-590, (July 29, 1991).
2. Corzine, R.H. Yan, and L.A. Coldren, "A Tanh Substitution Technique for the Analysis of Abrupt and Graded Interface Multi-Layer Dielectric Stacks," *J. of Quant. Elec.*, **27**, (9) 2086-2090, (September, 1991).
3. Corzine and L.A. Coldren, "Design of Low Threshold, High Output Power DBR Surface-Emitting Lasers," *IEEE LEOS'91*, San Jose, CA, paper no. SDL4.1, (November 4-7, 1991).
4. Yi, N.Dagli, and L.A. Coldren, "Investigation of Tilted Superlattices for Quantum Wire Laser Applications," *Appl. Phys. Lett.*, **59**, (23), 3015, (December 2, 1991).
5. J.A. Skidmore, G.D. Spiers, J.H. English, Z. Xu, D.L. Green, D.B. Young, L.A. Coldren, E.L. Hu, P.M. Petroff, C.B. Prater, and P.K. Hansma, "In-Situ Processing of GaAs/AlGaAs by Low Damage Selective Etching and Focussed Ion Beam Patterning," *LEOS Summer Topical '91*, Newport Beach, CA, paper no. THB.3, (July 31 - August 2, 1991).
6. C.P. Chao, S.Y. Hu, P. Floyd, K-K. Law, S.W. Corzine, J.L. Merz, A.C. Gossard, and L.A. Coldren, "Fabrication of Low-Threshold InGaAs/GaAs Ridge Waveguide Lasers by using *In Situ* Monitored Reactive Ion Etching," *Photonics Tech. Letts.*, **3**, (7) 585-587, (July, 1991).
7. K-K. Law, M. Whitehead, J.L. Merz, and L.A. Coldren, "Simultaneous Achievement of Low Insertion Loss, High Contrast and Low Operating Voltage in Asymmetric Fabry-Perot Reflection Modulator," *Electron. Lett.*, **27**, (20), 1863- 1865, (September 26, 1991).
8. R.S. Geels, S.W. Corzine, B. Thibeault and L.A. Coldren, "Efficient Vertical-Cavity Surface-Emitting Lasers with Useful Outputs to over 100°C," *OFC'92*, San Jose, CA, paper no. WB3, (February 3-7, 1992).
9. L.A. Coldren, R.S. Geels, S.W. Corzine and J.W. Scott, "Efficient Vertical-Cavity Lasers," *Optical and Quantum Electronics*, special issue **24**, S105-S119, (1992). INVITED PAPER
10. K-K. Law, M. Whitehead, J.L. Merz, and L.A. Coldren, "High Performance Quantum Well Asymmetric Fabry-Perot Reflection Modulators: Effect of Layer Thickness Variations," *MRS '92 Fall Meeting Proceeding*, **240**, 609-614, (1992).
11. C.C. Barron, M. Whitehead, K-K. Law, J.W. Scott, M.E. Heimbuch and L.A. Coldren, "K-Band Operation of Asymmetric Fabry-Perot Modulators," *Photonics Tech. Ltrs.*, **4**, (5) (May, 1992).
12. J.A. Skidmore, G.D. Spiers, J.H. English, Z. Xu, Y.J. Li, C.B. Prater, L.A. Coldren, E.L. Hu and P.M. Petroff, "Low Damage Anisotropic Radical-Beam Ion-Beam Etching and Selective Chemical Etching of Focused Ion Beam-Damaged GaAs Substrates," *SPIE'92*, San Jose, CA, paper no. 1671-37, (1992).
13. S.W. Corzine and L.A. Coldren, "Theoretical Gain in Strained-Layer Quantum Wells," *SPIE Symposium'93*, (1993). INVITED PAPER
14. S.Y. Hu, D.B. Young, A.C. Gossard, and L.A. Coldren, "The Effect of Lateral Leakage Current on the Experimental Gain/Current-Density Curve in Quantum-Well Ridge-Waveguide Lasers," submitted to *J. of Quant. Elect.*, (1993).
15. S.Y. Hu, M.S. Miller, D.B. Young, J.C. Yi, D. Leonard, A.C. Gossard, P.M. Petroff, L.A. Coldren, and N. Dagli, "Optical Gain Anisotropy in Serpentine Superlattice Nanowire-Array Lasers," *Applied Physics Ltrs.*, **63**, (15), 2015-2017, (October, 11, 1993).

16. D.B. Young, S.W. Corzine, F.H. Peters, J.W. Scott, B.J. Thibeault, and L.A. Coldren, "Constant-Threshold, High-Power Vertical-Cavity Surface-Emitting Lasers," *IEEE LEOS '92*, paper no. DLTA13.4, Boston, MA (November 15-20, 1992).
17. D.B. Young, D.I. Babic, S.P. DenBaars, and L.A. Coldren, "Epitaxial AlGaAs/AlAs Distributed Bragg Reflectors for Green (550nm) Lightwaves," *Electronic Letters*, 28, (20) 1873-1874, (September 24, 1992).
18. D.B. Young, J.W. Scott, F.H. Peters, B.J. Thibeault, S.W. Corzine, M.G. Peters, S.-L. Lee and L.A. Coldren, "High-Power Temperature-Insensitive Gain-Offset InGaAs/GaAs Vertical-Cavity Surface-Emitting Lasers," *Photonics Tech. Letters*, 5, (2), 129-132, (February, 1993).
19. D.B. Young, J.W. Scott, F.H. Peters, M.G. Peters, M.L. Majewski, B.J. Thibeault, S.W. Corzine, and L.A. Coldren, "Enhanced Performance of Offset-Gain High-Barrier Vertical Cavity Surface Emitting Lasers," *J. of Quantum Electronics*, Special Issue, 29, (6), 2013-2022, (June, 1993).
20. S.Y. Hu, M.S. Miller, D.B. Young, J.C. Yi, D. Leonard, A.C. Gossard, P.M. Petroff, L.A. Coldren, and N. Dagli, "Optical Gain Anisotropy in Serpentine Superlattice Nanowire-Array Lasers," *Applied Physics Ltrs.*, 63, (15), 2015-2017, (October 11, 1993).
21. D.S.L. Mui, T.A. Strand, B.J. Thibeault, L.A. Coldren, P.M. Petroff, and E.L. Hu, "Characteristics of In-Situ Cl<sub>2</sub> Etched/Regrown GaAs/GaAs Interfaces," *37th International Symposium on Electron, Ion, and Photon Beams*, San Diego, CA, poster no. C14, (June 1-4, 1993). And *J. Vac. Sci. Tech. B*, 11, (6), 2266-2269, (November/December 1993).